MECHANIKA
TEORETYCZNA
I STOSOWANA
1-2, 28 (1990)

STRENGTH ANALYSIS OF MULTI-ROPE WINDING MACHINE DRUM DRIVE

STEFAN BUĆKO (KRAKÓW)

1. Introduction

Multi-rope drum drive becomes one of the basical sets in the vertical winding machines in deep mines. In contemporary solutions a drum drive is constructed as a cylindrical shell stiffened with internal circular ribs and closed by two radially ribbed circle plates connected with a main shaft - Fig. 1. The connection between the shell and the side plates has a character of an elastic restraint - a tendency to increase a flexibility of that joint has been observed lately.

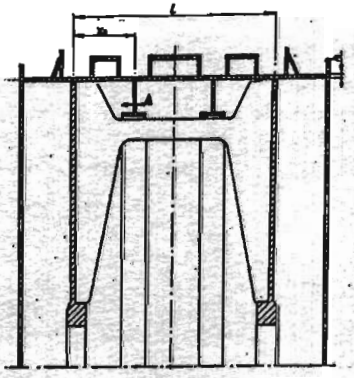

Fig. 1.

Up-to-date calculation methods basing on a model of orthotropic shell (constructional orthotropy as a result of washout-redistribu- tion of circular ribs) as well as a reduced thickness of the shell are taken into account, this enables to determine the local stress states in internal ribs zones.

In the paper a method of stress and strain states analysis in the drum drive shell, with regards to a local influence of circular ribs, as well as a method of strength analysis of a smooth shell in terms of loading have been presented.

Similar problems were investigated by Skalmierski (1963) who applied double Fourier series in the form proposed by W. Flügge to Goldenveizer's

equations.

The essential differences between this work and the above paper are: the equilbrium equations of shell and distribution of loadings, approximation of real loadings by certain continuous loadings this results also in a better convergence of series. The good convergence of the solution makes it possible to calculation of displacements, stresses and boundary forces.

2. Scheme of the proposed method of stress analysis in a drum drive shell

The proposed method enables stress and strain states analysis in the elastic cylindrical shell with simply supported edges, with clamped edges as well as in a shell with elastically fixed edges.

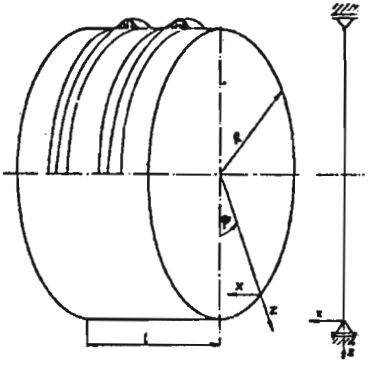

Fig.2.

On the present stage of the analysis the computational model has been considered in form of a shell with simply supported edges locally loaded by contact pressure of a lifting rope -Fig.2. For the applied ratios of dimensions the differences in shell edges bearing have no essential influence upon the maximum effort in the shell.

In the analysis the following distribution of contact pressures from lifting rope on a width 's' has been taken: constant with reference to variable ϕ (for range $\frac{\pi}{2} \leq \phi \leq \frac{3}{2}\cdot\pi$) and sinusoidally varying along to x axis. It is difficult to describe a distribution of pressure with respect to x axis since the pressure from rope is transmitted through wedge shaped pads made of rubberlike material of width about 100 mm. Pressure variation independent of angle ϕ corresponds to neglecting the influence of a driving moment - moment that results in stress $\tau < 1.0$ MPa in shell.

Displacements equilibrium equations for the shell according to Flügge

(1972) are the following:

$$
\begin{aligned}
&R^2\cdot u'' + \frac{1-\nu}{2}\cdot\ddot{u} + \frac{1+\nu}{2}\cdot R\cdot\dot{v}' + \nu\cdot R\cdot w' + \frac{p_x\cdot R^2}{D} = 0 \ ,\\
&\frac{1+\nu}{2}\cdot R\cdot\dot{u}' + \ddot{v} + \frac{1-\nu}{2}\cdot R^2\cdot v'' + \dot{w} + \frac{p_\phi\cdot R^2}{D} = 0 \ ,\\
&\nu\cdot R\cdot u' + \dot{v} + w + k\cdot(R^4\cdot w'''' + 2\cdot R^2\cdot w'' + \ddot{w}) - \frac{p_z\cdot R^2}{D} = 0 \ ,
\end{aligned}
\qquad (2.1)
$$

$$
[\,]' = \frac{\partial(\,)}{\partial x} \ , \quad [\,]^{\cdot} = \frac{\partial(\,)}{\partial\phi} \ , \quad D = \frac{E\cdot h}{1-\nu^2} \ , \quad k = \frac{h^2}{12\cdot R^2} \ , \quad K = \frac{E\cdot h^3}{12(1-\nu^2)} \ .
$$

u, v, w -displacements; R -radius of midsurface; h -shell thickness; E-Young's modulus; ν -Poisson's ratio.

Boundary conditions correspond to the pivot-bearings of the both edges of the shell in the thin stiff disks and have the following form:

$$
\begin{aligned}
&w(0,\phi)=0,\ w''(0,\phi)=0,\ v(0,\phi)=0,\ N_x(0,\phi)=0 \text{ or } u'(0,\phi)=0 \ ,\\
&w(l,\phi)=0,\ w''(l,\phi)=0,\ v(l,\phi)=0,\ N_x(l,\phi)=0 \text{ or } u'(l,\phi)=0 \ .
\end{aligned}
\qquad (2.2)
$$

For the assumed boundary condition on the both edges the following forces appear:

S_z - force normal to the midsurface,

S_ϕ - force tangential to the midsurface and to the plate.

$$
S_z = \left[Q_x + \frac{1}{R}\cdot\dot{M}_{x\phi} \right]_{\substack{x=0\\x=l}} = \left[\frac{1}{R}\cdot M_x' + \frac{2}{R}\cdot\dot{M}_{x\phi} \right]_{\substack{x=0\\x=l}} \ ,
$$

$$
S_\phi = \left[N_{x\phi} - \frac{1}{R}\cdot M_{x\phi} \right]_{\substack{x=0\\x=l}} \ . \qquad (2.3)
$$

The sum of vertical components of S_z and S_ϕ forces should equate acting forces - i.e. forces from rope pull.

Solution of the set of equations (2.1) with boundary conditions (2.2) could be taken as:

$$
u = \sum_{m=1}^{\infty}\sum_{n=0}^{\infty} B_{mn}\cdot\cos\frac{m\pi x}{l}\cdot\cos n\phi \ , \qquad v = \sum_{m=1}^{\infty}\sum_{n=1}^{\infty} C_{mn}\cdot\sin\frac{m\pi x}{l}\cdot\sin n\phi \ , \qquad (2.4)
$$

$$w = \sum_{m=1}^{\infty}\sum_{n=0}^{\infty} D_{mn}\cdot\sin\frac{m\pi x}{l}\cdot\cos n\phi \ ,$$

where according to the symetry m = 1,3,5,...

Coefficients of series (2.3) were found by substitution of expansion of loadings in Fourier series to (2.1)

$$p_x = p_\phi = 0 \ , \quad p_z = \sum_{m=1,3,5}^{\infty}\sum_{n=0,1,3}^{\infty} A_{mn}\cdot\sin\frac{m\pi x}{l}\cdot\cos n\phi \ , \tag{2.5}$$

and by comparison of coefficients.

Finally the following relations were found:

$$D_{mn} = A_{mn}\cdot\bar{D}_{mn} \ , \quad B_{mn} = A_{mn}\cdot\bar{B}_{mn} \ , \quad C_{mn} = A_{mn}\cdot\bar{C}_{mn} \ , \tag{2.6}$$

where $\bar{D}_{mn}$, $\bar{B}_{mn}$, $\bar{C}_{mn}$ are functions of m,n as well as geometrical and physical parameters of the shell.

$$\bar{D}_{mo} = \frac{R^2}{D}\cdot\frac{1}{1-\nu^2 + k\cdot\frac{\pi^4\cdot R^4}{l^4}\cdot m^4} \qquad \text{for } n = 0 \ ,$$

$$\bar{D}_{mn} = \frac{1}{\left(\frac{2-\nu-\nu^2}{1+\nu}\cdot\frac{\pi R}{l}m + \frac{1-\nu}{1+\nu}\cdot\frac{l}{\pi R}\cdot\frac{n^2}{m}\right)F_{mn} + \left[1-\frac{2\cdot\nu}{1+\nu}+k\left(\frac{\pi^4R^4}{l^4}m^4+2\frac{\pi^2R^2}{l^2}m^2n^2+n^4\right)\right]} \tag{2.7}$$

$$\text{for } n = 1,2,3... \ ,$$

$$\bar{B}_{mo} = \frac{1}{\pi\cdot R}\cdot\frac{\nu}{m}\cdot D_{mo} \qquad \text{for } n = 0 \ ,$$

$$\bar{B}_{mn} = \bar{D}_{mn}\cdot F_{mn} \qquad \text{for } n = 1,2,3... \ , \tag{2.8}$$

$$\bar{C}_{mn} = \bar{D}_{mn}\left(\frac{2}{1+\nu}\cdot\frac{\pi R}{l}\cdot\frac{m}{n}\cdot F_{mn} + \frac{1-\nu}{1+\nu}\cdot\frac{l}{\pi R}\cdot\frac{n}{m}\cdot F_{mn} - \frac{2\cdot\nu}{1+\nu}\cdot\frac{1}{n}\right) \qquad n=1,2,3... \ , \tag{2.9}$$

$$F_{mn} = \frac{\nu\cdot\frac{\pi^2\cdot R^2}{l^2}\cdot\frac{m^2}{n^2} - n}{2\cdot\frac{\pi\cdot R}{l}\cdot m\cdot n + \frac{l}{\pi\cdot R}\cdot\frac{n^3}{m} + \frac{\pi^3\cdot R^3}{l^3}\cdot\frac{m^3}{n}} \ . \tag{2.10}$$

In this way , displacements u,v,w, internal forces and external edge loadings have been derived for the smooth shell.

3. Analysis of the influence of circular ribs on stress and strain states.

The basis of the analysis is the assumption, that the forces of mutual interaction appear between the shell and the ribs which could be treated as additional loading of the smooth shell. The rib pressure on the shell has been taken as a function partially constant with reference to variable x:

$$q_s = \frac{1}{\Delta} \cdot T_z(\phi) \ , \qquad T_z(\phi) = \sum_{n=0}^{\infty} T_n \cdot \cos n\phi \ , \tag{3.1}$$

when Δ - rib width at the connecting place with the shell.

Loading q_s could be shown as:

$$q_s = \sum_{m=1}^{\infty} \sum_{n=0}^{\infty} a_{mn} \cdot \sin \frac{m\pi x}{l} \cdot \cos n\phi \ , \tag{3.2}$$

(m=1,3,5..., for symetrically distributed ribs).

Coefficients of series (3.1) and (3.2) can be calculated from the compatibility condition of displacements of both the shell and ribs $w_r(\phi)$ along circumference of circle in the middle of the rib width ($x=x_s$)

$$w(x_s, \phi) = w_r(\phi) \ . \tag{3.3}$$

Taking the criterion (3.3) and the radial direction of force $T_z(\phi)$ is equivalent to neglecting the torsional stiffness of the rib. When introducing finite width of the rib ($\Delta \neq 0$) one can improve convergence of the solutions -for $\Delta=0$, $\frac{1}{m}$ is eliminated what impairs the convergence.

For two ribs of width Δ distributed at the distance x_s from the edges, the solution has a form:

$$q_s = \frac{4}{\pi\Delta} \cdot \sum_{m=1,3}^{\infty} \sum_{n=0,2,3}^{\infty} \frac{1}{m} \cdot T_n \cdot \sin \frac{m\pi x_s}{l} \cdot \sin \frac{m\pi\Delta}{l} \cdot \sin \frac{m\pi x}{l} \cdot \cos n\phi \ ,$$

$$T_0 = \frac{\sum_{m=1,3}^{\infty} A_{m0}\cdot\bar{D}_{m0}\cdot\sin\frac{m\pi x}{l}}{\frac{R^2}{E\cdot F} + \frac{4}{\pi\Delta}\cdot\sum_{m=1,3,}^{\infty}\frac{1}{m}\cdot\bar{D}_{m0}\cdot\sin^2\frac{m\pi x_s}{l}\cdot\sin\frac{m\pi\Delta}{l}} \quad \text{for } n=0\ , \qquad (3.4)$$

$$T_n = \frac{\sum_{m=1,3}^{\infty} A_{mn}\cdot\bar{D}_{mn}\cdot\sin\frac{m\pi x}{l}}{\frac{R^4}{EI(n^2-1)} + \frac{4}{\pi\Delta}\cdot\sum_{m=1,3,}^{\infty}\frac{1}{m}\cdot\bar{D}_{mn}\cdot\sin^2\frac{m\pi x_s}{l}\cdot\sin\frac{m\pi\Delta}{l}} \quad \text{for } n=2,3,4\ldots\ ,$$

F, I -area and inertial moment of the cross section of the rib

Displacements $u_s(x,\phi)$, $v_s(x,\phi)$ have an analogous form to (2.4). The total displacements and internal forces in the shell with circular ribs can be derived by superposition of displacements and internal forces from acting loading and interaction forces from ribs.

4. Possibilities of application of the method for another boundary conditions and loadings

Series (2.1) being the solution of the set of equations (2.1) satisfy automatically simply supported boudary conditions (2.2). Without the change of the form of the solution one can get, by superposition, a solution for stiff and elastic clamping of the edges.

Solution for stiffy-fixed shell could be obtained by applying moment $M_n = \sum M_n\cdot\cos n\phi$, where coefficients are derived from the following condition:

$$w'_q(0,\phi) + w'_u(0,\phi) = 0\ , \qquad (4.1)$$

w_q - shell displacements from active forces,

w_u - shell displacements from moment M_u.

For more complex loadings, i.e. where the condition of parity with reference to ϕ is necessary to consider more general form of solution:

$$w = \sum_{m=1}^{\infty}\sum_{n=0}^{\infty} K_{mn}\cdot\sin\frac{m\pi x}{l}\cdot\cos n\phi + \sum_{m=1}^{\infty}\sum_{n=1}^{\infty} L_{mn}\cdot\sin\frac{m\pi x}{l}\cdot\sin n\phi\ , \qquad (4.2)$$

A sequence of sets up of 9 equations with 9 unknowns each must be solved while deriving coefficients of series of (4.2) type.

5. Example

Numerical calculations for 5 different types of shell constructions, including the real shell of 4-rope drum drive working in the cole-mine "Halemba" (height of lifting 1028m), have been done to prove the correctness of the proposed method of strength calculation for drum drive shell as well as to enable the comparative analysis of the construction. The real drum drive has two circumferential internal ribs (Fig.1) - two outer ropes were placed on the side-disks.

The basic constructional parameters of the real shell are: R=2.6 [m], l=1.35 [m], x_s=0.45 [m], h=25 [mm]; F=1.05·10^{-2} [m^2], I=1.15·10^{-4} [m^4] - area and inertial moment at the cross section of the rib; N=0.263 [MN] - average force in the rope; E=2·10^5 [MPa], ν=0.3 .

Calculations were done for shells given below for certain values of R, l, x_s and N, E, ν:

a. real shell,
b. smooth shell of thickness h=25 mm,
c. smooth shell of thickness h=35 mm,
d. shell of thickness h=25 mm reinforced with 1 pair of ribs of parameters F_1=6·10^{-3}m^2, I_1=5·10^{-6}m^4,
e. shell of thickness h=30 mm reinforced with 1 pair of ribs of parameters F_1 , I_1 .

In calculations an influence of external ribs (necessary for proper guidance of ropes) - taking into consideration their influence in circumferential direction corresponds to the increase of shell thickness of about 5 mm (for dimentions of the real construction).

Before final calculations the examination of the convergence of the solution were done. A good convergence of the obtained formulas has been shown. That is a result of the taken schemes of loadings (according to the idea of the method) - for loadings assumed by Skalmierski (1963) the

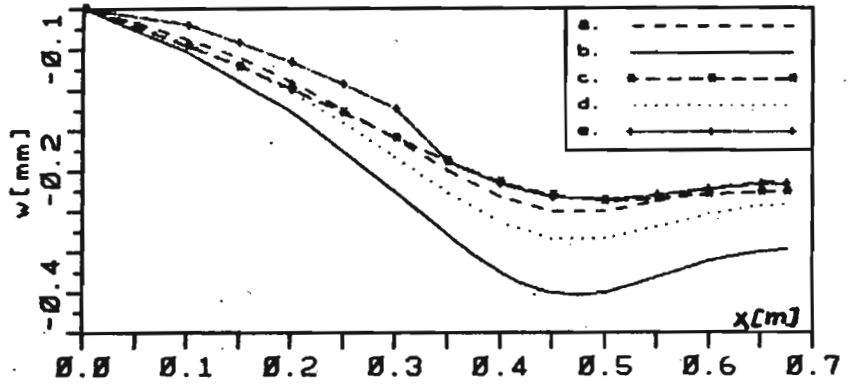

Fig.3. Deflection w -generating line.

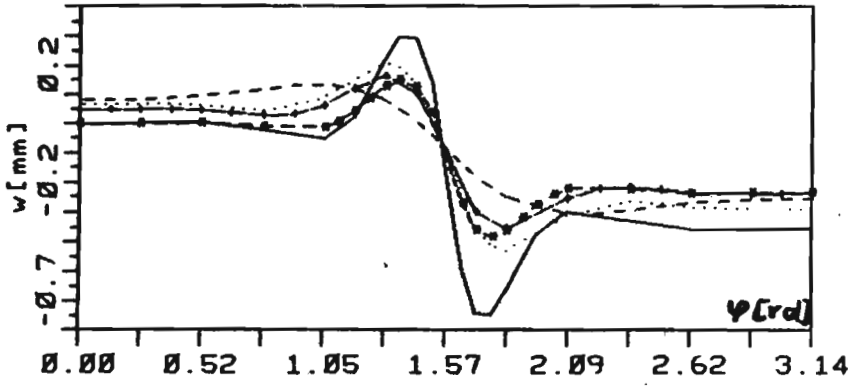

Fig.4. Deflection w at the circumference under the rope.

convergence is worse and for transverse forces problematical.

The results of calculations are given in a form of graphs of functions of: deflection $w(x,\pi)$, $w(x_s,\phi)$, stresses $\sigma_x^o = \frac{N_x}{h}$, $\sigma_\phi^o = \frac{N_\phi}{h}$, $\tau_{x\phi}^o = \frac{N_{x\phi}}{h}$, $\sigma_x^g = \frac{6M_x}{h^2}$, $\sigma_\phi^g = \frac{6M_\phi}{h^2}$, for $x=x_s$ (circuit under the rope) as well as graphs of boundary forces.

TABLE 1.

ver.	σ_{omax} [MPa]	w_{max} [mm]
a	32.5	0.30
b	48.0	0.49
c	29.0	0.38
d	32.0	0.43
e	29.0	0.25

To make the comparision easier tab.1 gives a set up of maximum reduced stresses σ_0 (acc. to Huber) and maximum values of radial displacements.

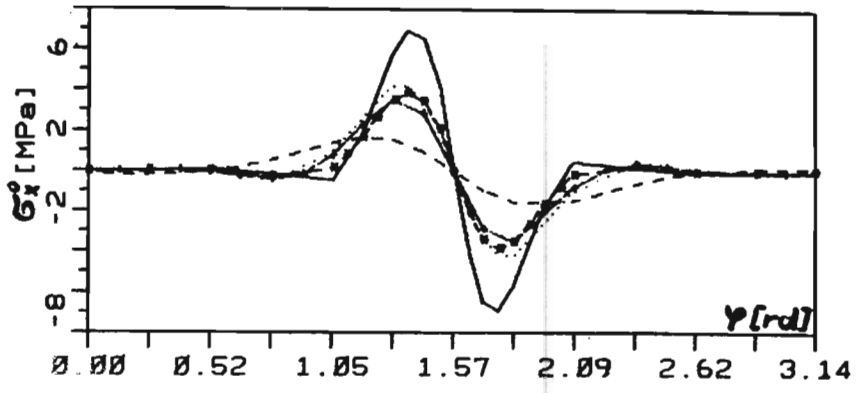

Fig.5. Stress σ_x° at the circumference under the rope.

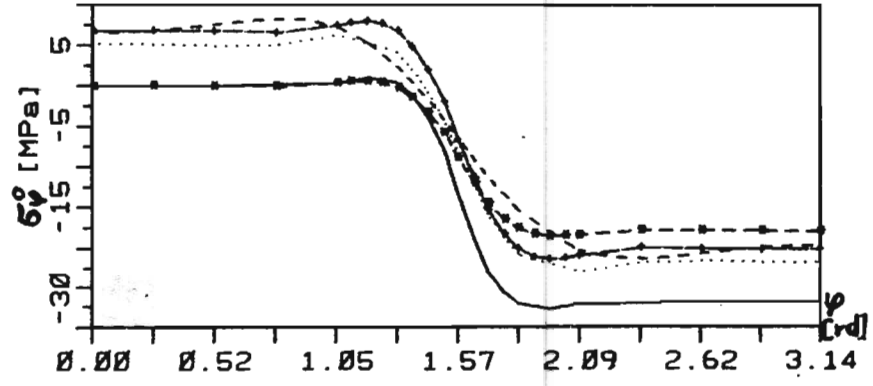

Fig.6. Stress σ_ϕ° at the circumference under the rope.

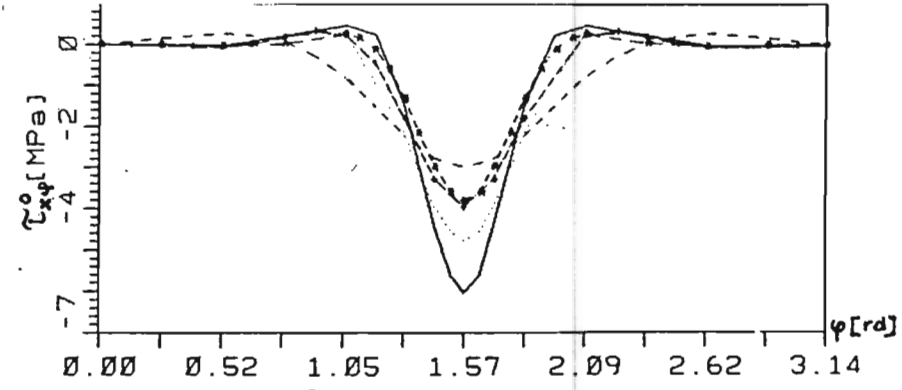

Fig.7. Stress $\tau_{x\phi}^\circ$ at the circumference under the rope.

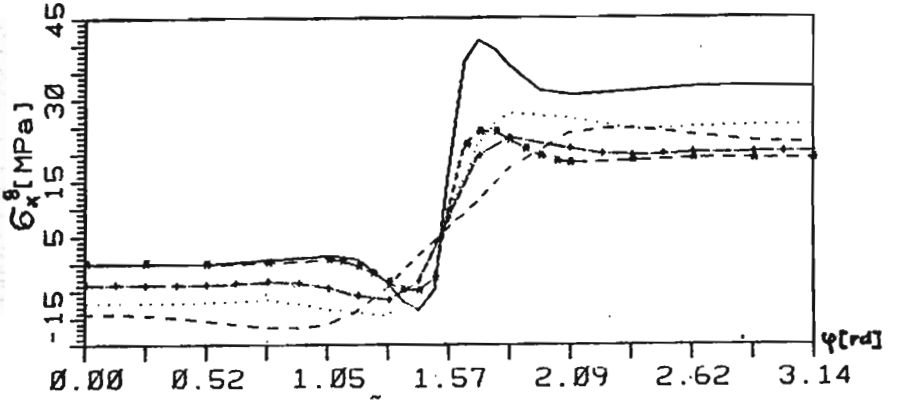

Fig.8. Stress σ_x^9 at the circumference under the rope.

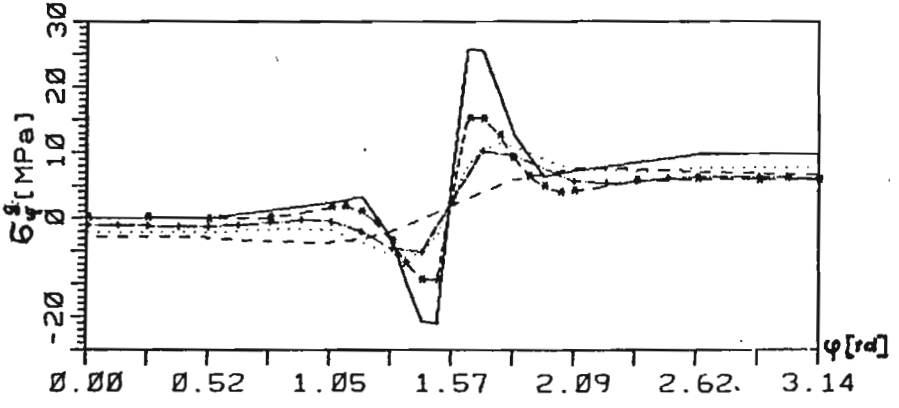

Fig.9. Stress σ_ϕ^9 at the circumference under the rope.

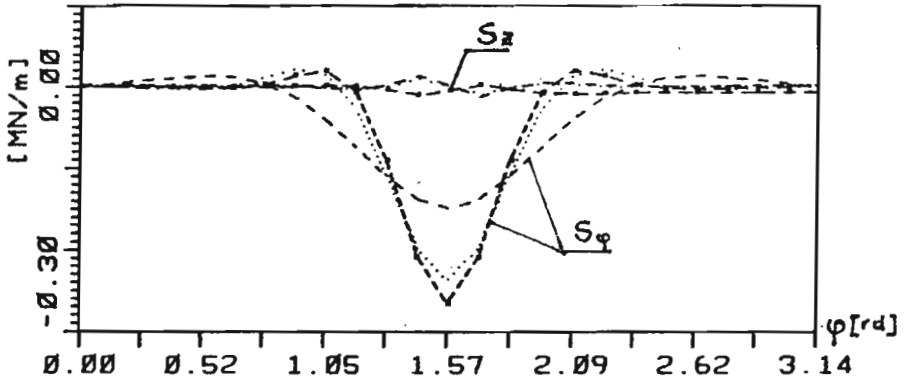

Fig.10. Boundary forces.

6. Discusion and conclusions

Rigid displacement of the intersection $x=x_s$, influenced by the rib, can be clearly noticed for the real shell deformations. For smooth shells in their lower part displacements and stresses are small and for range $-\frac{\pi}{3} \leq \phi \leq \frac{\pi}{2}$ practically are equal zero. The change in the way of vertical forces transmition is observed - when moving from the rope to the disk shear forces decrease fast while tangential $N_{x\phi}$ increase around $\phi = \frac{\pi}{2}$. The influence of internal ribs results in the shift of stress spectrum from pulsating one (starting from zero; for smooth shell) towards smetrical cycle.

Strain gauges experiments conducted for similar construction showed the values of stresses about 15-20% less then calculated - it should be explained by the influence of external ribs.

Conclusions:

1. Analysis of results, comparison with accesible -not complete- experimental data and good convergence of the solution motivate the usefulness of the proposed method for constructional works.
2. C, d and e constructions show an effort not bigger than for working construction. It points out the possibility of building a simpler technologically drum drive of the same reliability.
3. Boundary forces of the shell indicate that forces tangential to the circuit of side-plates become their basic loadings -it could bbe a basis of constructional analysis of side-plates.

References

Bucko, S., Zieliński, A. (1975): Analiza konstrukcji bębna płuczki do płukania kamienia wapiennego, *Zesz. Nauk. Pol. Łódz.* 10

Flügge, W. (1972): Powłoki - obliczenia statyczne, Arkady, W-wa

Popowicz, O. (1964): Maszyny wyciągowe-bębny i koła... Gliwice

Skalmierski, B. (1963): Problemy statyki i dynamiki powłok użebrowanych, *Zeszyt Nauk. Pol. Śląskiej, Mechanika* z. 10.

Summary

ANALIZA WYTRZYMAŁOŚCIOWA WIELOLINOWEGO BĘBNA PĘDNEGO MASZYNY WYCIĄGOWEJ.

W pracy przedstawiono metodę analizy odkształceń i naprężeń w powłoce bębna maszyny wyciągowej. Równania równowagi powłoki (w/g W.Flügge) rozwiązano przy pomocy podwójnych szeregów Fouriera. Metoda pozwala na analizę powłoki gładkiej i wzmocnionej żebrami obwodowymi. W oparciu o wyprowadzone wzory wykonano obliczenia dla kilku konstrukcji bębna. Wyniki obliczeń wskazują na możliwość uproszczenia konstrukcji bębna bez obniżenia wytrzymałości.